analytica

MDPI

Article

Evaluation of the Ellman's Reagent Protocol for Free Sulfhydryls Under Protein Denaturing Conditions

Sophia R. Ginet [1,†], Frank Gonzalez [1,†], Maxine L. Marano [1,†], Megha D. Salecha [1], Joseph E. Reiner [2] and Gregory A. Caputo [1,*]

[1] Department of Chemistry and Biochemistry, Rowan University, Glassboro, NJ 08028, USA; ginets35@rowan.edu (S.R.G.); gonzal108@students.rowan.edu (F.G.); marano35@students.rowan.edu (M.L.M.); salech97@rowan.edu (M.D.S.)
[2] Department of Physics, Virginia Commonwealth University, Richmond, VA 23284, USA; jereiner@vcu.edu
* Correspondence: caputo@rowan.edu
† These authors contributed equally to the work.

Abstract: Early detection of cancer can dramatically improve long-term prognosis and survivability in a variety of different cancer types. However, for many cancer types, the ability to effectively detect early-developing tumors is challenging, especially in physiological locations with limited visibility or access. Previously, we reported a sensing platform and methodology to detect biomarker peptides found in urine from ovarian cancer patients. This sensing platform relies on peptide interactions with gold nanoclusters through thiol-mediated linkages; thus, the sensitivity of the biomarker assay is directly related to appropriate redox states of the biomarkers in question. Here, we report on an expansion of the traditional thiol-reactivity assay originally developed by Ellman to include and evaluate a variety of solution modifications that may be used in conjunction with the biomarker-sensing platform. Because biomarker peptides may be isolated from a variety of biological tissues or fluids, depending on the target condition or disease, we screened numerous solution conditions that may be directly used in sample preparation and peptide extraction. The data demonstrate that the assay maintains linearity under these various conditions. The assay was then applied to a variety of models and biomarker peptides and exhibits the expected linear response. These results demonstrate the applicability of the thiol-reactivity assay to biologically derived samples, and the flexibility to ensure sample preparation and treatment will retain the appropriate sample redox conditions to ensure optimal interactions with the biosensor platform. It also facilitates the ability to perform quality control on clinically derived biological samples to ensure appropriate preparations, and concentrations are available for application to the nanopore biosensor platform.

Keywords: peptide biomarkers; cysteine reactivity; sulfhydryl reactivity

check for updates

Academic Editor: Marcello Locatelli

Received: 10 April 2025
Revised: 6 May 2025
Accepted: 8 May 2025
Published: 13 May 2025

Citation: Ginet, S.R.; Gonzalez, F.; Marano, M.L.; Salecha, M.D.; Reiner, J.E.; Caputo, G.A. Evaluation of the Ellman's Reagent Protocol for Free Sulfhydryls Under Protein Denaturing Conditions. *Analytica* **2025**, *6*, 18. https://doi.org/10.3390/analytica6020018

Copyright: © 2025 by the authors. Licensee MDPI, Basel, Switzerland. This article is an open access article distributed under the terms and conditions of the Creative Commons Attribution (CC BY) license (https://creativecommons.org/licenses/by/4.0/).

1. Introduction

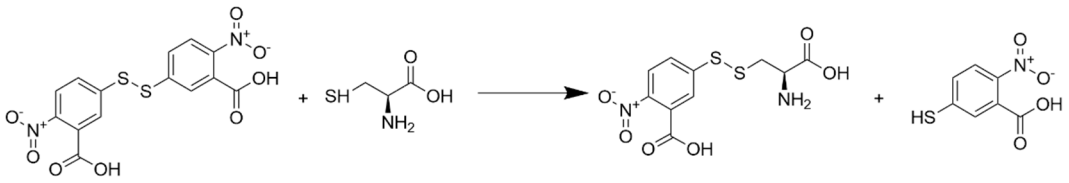
Biomarkers are biomolecules that are indicative of some cellular state or process and are most often used as indicators for diseases or health-related conditions. Biomarkers can be any form or class of biomolecules, including proteins, sugars, nucleic acids, or small-molecule metabolites [1–5]. Numerous biomarkers have been identified for a wide variety of conditions, including Alzheimer's disease, viral infections [1,6], stress-related illnesses [7], and multiple types of cancers [8–10]. Biomarkers are not only used in the identification of a disease state but can also be used to identify sensitivity or response to specific treatments for those diseases [11–13]. These ongoing identifications

of biomarkers have also yielded multiple repositories for biomarker classification and organization [14–16].

One of the major driving factors in the interest and exploration of biomarkers is the need for early diagnosis of diseases. Specifically, early diagnosis of cancers has received tremendous interest across all types of cancers [17–19]. Statistics on survival rates indicate that some cancers have over 95% five-year survival rates if diagnosed early during Stage 1 [17–19]. Based on data from the UK over the period 2014–2018, those survival rates drop to between 70% for breast and skin cancers to as low as ~30% for ovarian cancers when detected in Stage 3. Across all types of cancer, late detection in Stage 4 yields lower than 30% five-year survival rates. These trends are paralleled in other regions across the world as well [17]. While the trend holds across all cancers, another striking example is colon cancer, which has >90% five-year survival rate if detected in Stage 1, which drops to ~70% if detected in Stage 3 and below 20% if detected in Stage 4 [17]. Thus, there is a clear need for enhanced diagnostic tools and methods to detect cancers as early as possible.

Recently, we described a novel protein nanopore-based system for peptide detection [20,21]. This method relies on variations in current fluctuations across a protein nanopore embedded in a lipid bilayer. Peptides are introduced into the system and covalently bind to thiopronin-capped gold nanoclusters via disulfide bond formation. These disulfide-linked peptide-metallonanoclusters are then introduced into the pore, at which point they induce fluctuations in the current passing through the pore. These current fluctuations have been shown to be directly dependent on peptide length and are influenced by peptide sequence variations. Thus, the platform is ripe to be utilized in the identification of peptide biomarkers with cysteine (Cys) residues in their sequences. The end goal is to develop a robust, clinically deployed sensor device that can be utilized in the detection of disease-linked biomarkers isolated from biological fluids [20,21]. Because biomarker peptides may be isolated from a variety of biological tissues or fluids, depending on the target condition or disease, a variety of preparation protocols may be necessary to extract samples for analysis by the nanopore sensor. Additionally, as with all detection platforms, ensuring appropriate concentration of analytes in the sample is a critical requirement for effective operation of the sensor.

The Cys reactivity is key to the functionality of the platform described above. Cys residues can easily exist in both the oxidized and reduced forms and are commonly found in both forms in biological systems. In biochemical, in vitro systems, cysteine reactivity is frequently assessed by use of "Ellman's reagent", 5,5′-dithiobis-(2-nitrobenzoic acid) (DTNB), (Scheme 1). This compound reacts with free sulfhydryl groups on Cys, forming a mixed-disulfide product and generating a chromogenic product, thus allowing a direct assessment of free Cys concentration using visible absorption spectroscopy [22]. Despite several other assays existing [23,24], the DTNB-based assay is the standard in the field, including applications to non-biological samples and to surface-modified nanoparticles [25–27]. Nonetheless, there are several limitations to the assay regarding chemical incompatibility with oximes, basic pH, and general issues in complex biological samples [28,29].



Scheme 1. Reaction of 5,5′-dithiobis-(2-nitrobenzoic acid) (DTNB, Ellman's Reagent) with free cysteine.

In order for the nanopore sensor system to yield accurate results, the samples must be in the appropriate state for analysis. Many biomarkers are proteins, which require denaturation and digestion by proteases before application to the described nanopore

sensor. Similarly, some proteins may require denaturation by chaotropes, such as urea or guanidine HCl, to allow proteolytic digestion or reduce aggregation in solution. As the nanopore system described relies on Cys–gold interactions to tether the peptides, appropriate oxidation state of the Cys-containing biomarker is critical and must withstand the conditions required for sample preparation. More broadly, there has been limited data regarding the applicability of the DTNB or Ellman's reagent method to a broader set of conditions [30]. In this manuscript, we demonstrate that the DTNB assay is robust in maintaining linearity under a variety of solution conditions and yields linear output when analyzing small- to medium-length peptides. This will allow the assay to be used in conjunction with various potential sample preparation routines for nanopore analysis.

2. Materials and Methods

2.1. Materials

All reagents were from VWR (Radnor, PA, USA) or Sigma-Aldrich (St Louis, MO, USA) and used as provided. Reducing gel functionalized with tris(2-carboxyethyl)phosphine) (TCEP) was from Thermo Scientific (Waltham, MA, USA). The primary assay buffer consisted of 100 mM sodium phosphate and 1 mM EDTA, pH 8.0. DTNB stock solutions were prepared in the pH 8 assay buffer at 10.1 mM (4 mg/mL) and stored in foil-covered tubes to prevent exposure to light. Stock solutions of L-cysteine were prepared by dissolving the amino acid in assay buffer to a final concentration of 1.5 mM. Other standards were made through serial dilution of this stock. Stock solutions of other amino acids (S-methylcysteine and D-methionine) and glutathione (both oxidized and reduced forms) were dissolved in 100 mM sodium phosphate and 1 mM EDTA, pH 8.0. The reducing agent dithiothreitol (DTT) was made as a 1 M stock solution in water and diluted as needed. Peptide stock solutions were dissolved to a final concentration of 1 mg/mL in 100 mM sodium phosphate and 1 mM EDTA, pH 8.0. Detergents cetyltrimethylammonium Bromide (CTAB) and dodium dodecyl sulfate (SDS) were made as 1 M stock solutions in DI water.

2.2. Absorbance Spectroscopy

The absorbance of the DTNB-Cys complex was measured at 412 nm. The assay was performed in large volumes (1 mL samples) using a Thermo Genesys UV-Vis instrument (Waltham, MA, USA) and a VWR UV-3100PC UV-Vis instrument. The reduced volume assay was performed in 96-well plates using a Molecular Devices MultiSkan M5 multimode plate reader (San Jose, CA, USA). Data is the average of at least five samples, and error bars represent the standard deviations of the data. Linear fitting of the data was performed using Microsoft Excel and the plugin Daniel's XL Toolbox [31].

3. Results

3.1. Reagent Stability and Assay Conditions

The long-term application of a Cys-specific nanopore-sensing platform in a clinical setting was the inspiration for the overall investigation. Keeping that in mind, the first question was if the DTNB solution was stable to freezing, a likely necessity if the required standardization components and reagents are to be delivered to a clinical site for application. This was investigated by preparing a stock solution of DTNB and splitting it between several tubes, all of which were frozen at −20 °C. A sample was removed from the freezer and thawed at room temperature after 4, 6, 8, 10, 12, and 14 days, at which point the DTNB stock was used in the standardization assay with L-cysteine as the molecule containing the sulfhydryl. The data is shown in Figure 1A. The data shows the expected linear correlation between absorbance and Cys concentration over all freezing durations. The variability within individual sampling time points was low, with standard deviation values being

>2 orders of magnitude smaller than the measurements. Some variability does occur in the samples at higher Cys concentrations, but the overall trendlines over the range of freezing time from 5 days up to 14 days only varies by a total of 0.2, with a standard deviation of fits being 0.07. While a relatively short period of time, this is promising for the development of long-lasting reagent mixtures for clinical deployment.

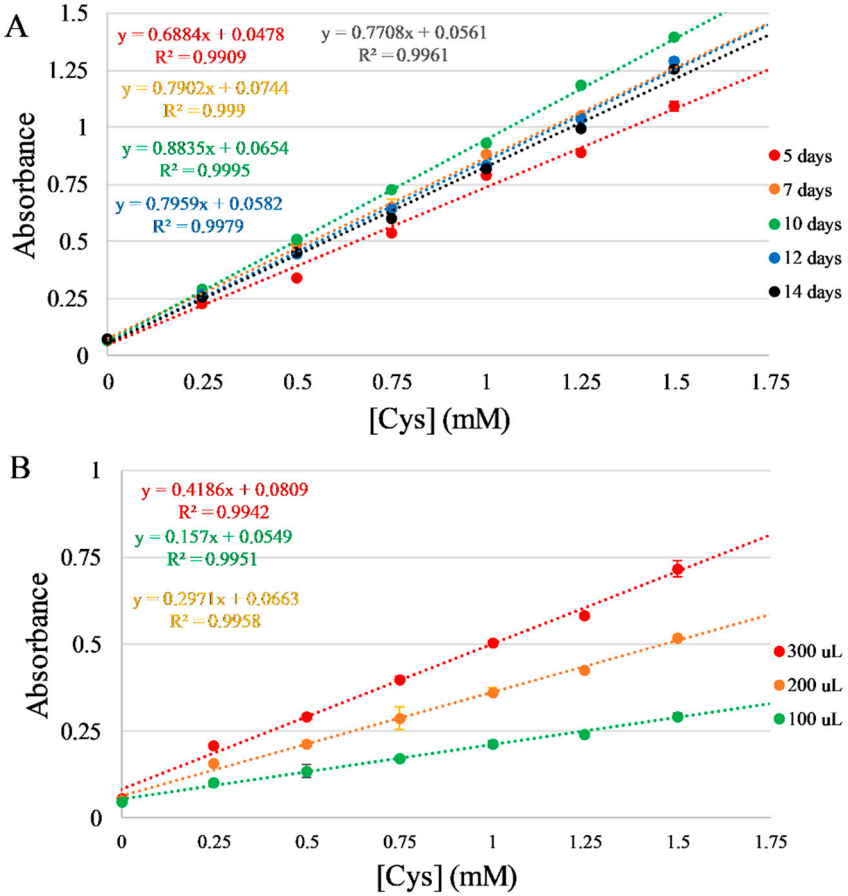


Figure 1. Experimental parameter evaluation for microplate assay. (**A**) Effect of freezing on DTNB reagent. Length of time the reagent was stored at −20 °C is shown in the legend. (**B**) Effect of sample volume on assay performance in microwell plates. For both panels, linear equations fit to the data and respective R^2 values are shown on the graphs and are color-coded corresponding to the data points. Error bars represent the standard deviation of at least 5 independent data points and are sometimes obscured by the data marker.

We next evaluated the assay volume and how this affected the output and sensitivity. With the goal of increasing sample throughput, we aimed to develop standard conditions that will maximize sample throughput and minimize reagent utilization, along with minimizing the need for the collected biological samples. As such, we analyzed the volume dependence of the assay in the 96-well format. This would be a critical piece in reducing the necessary working volume to increase throughput and minimize sample utilization. The results of this are shown in Figure 1B. The assay's linearity was maintained over the different sample volumes tested, but the slopes of the calibration decreased proportionally as sample volumes decreased. Representative absorbance spectra of DTNB alone and the same concentration of DTNB fully reacted with Cys are shown in Figure 2A. The spectra demonstrate a significant enhancement and red shift in the absorption peak of the DTNB in the 300–400 nm wavelength range upon reacting with Cys. The red-shifted peak exhibits a maximum at 410 nm, the wavelength chosen for the microplate assays. Similarly, representative spectra demonstrating the complete reaction of the DTNB with Cys are shown

in Figure 2B, where the DTNB-Cys samples were exposed to 1 mM DTT to reduce any unreacted materials. As shown by the spectra, DTT had no impact on the absorption peak, indicating the DTNB–Cys ratio was sufficient to fully react all DTNB in the sample.

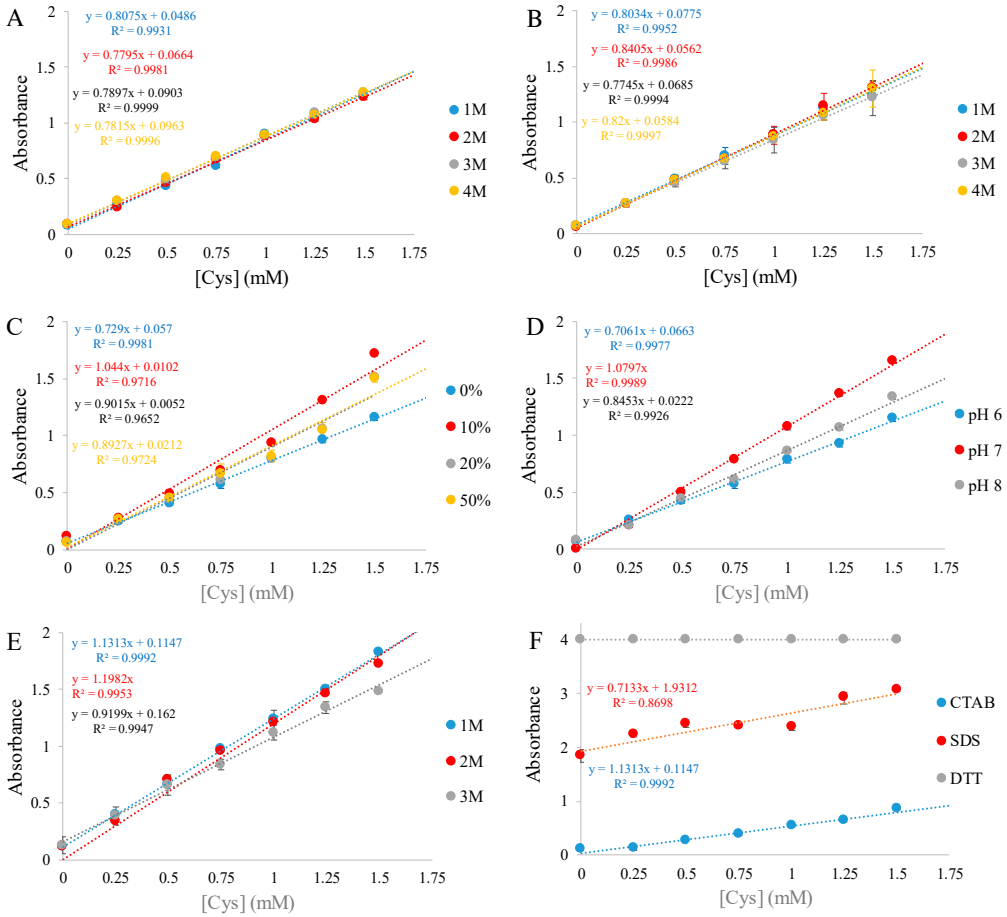


Figure 2. Effect of common denaturants on the DTNB–Cys reaction. (**A**) Guanidine hydrochloride, (**B**) urea, (**C**) ethanol, (**D**) varying solution pH values, (**E**) varying KCl concentration in the buffer, and (**F**) inclusion of 10 mM of the detergents CTAB or SDS or the reducing agent DTT. Linear fits and resulting fitting equations are correspondingly color-coded along with R^2 values of the fits. Data represent averages of at least 5 replicates, with error bars representing the standard deviation. In some cases, the error bars are smaller than the symbol size and are obscured.

3.2. Denaturants and Buffer Modifications

Considering that the goal of the nanopore-detection assay is to analyze peptides from complex biological samples, it is likely that some degree of sample preparation will be required prior to analysis. This preparation is likely to include buffer exchanges for compatibility with the sensor or the addition of denaturants to help solubilize and stabilize proteins in the complex mixture. As such, we examined the ability of the assay to perform under conditions where the pH is decreased as well as in the presence of common denaturating agents for protein samples—guanidine hydrochloride, urea, detergents, and ethanol. The results are shown in Figure 2. Overall, the assay retained linear response to Cys under all conditions tested. The protein denaturants guanidine hydrochloride (Figure 2A) and urea (Figure 2B) caused no detectable impact on the performance of the assay. There was a greater degree of variability in the samples in which varying concentrations of EtOH were included (Figure 2C), as well as those in which the assay pH was lowered to pH 7.0 and pH 6.0 (Figure 2D). However, there was no direct correlation between either of these components and the direction of the changes to the calibration curves. We also investigated

the impact of high salt concentrations on the assay, considering that the nanopore-sensing platform requires 3 M KCl for optimal current. Increasing the salt concentration had minimal effect on the assay, with 3 M KCl showing a slight decrease in sensitivity compared to 1 M and 2 M samples (Figure 2E). Supplementing the samples with the cationic detergent CTAB or the anionic detergent SDS did not affect the linearity of the calibration curves; however, SDS samples did exhibit an increased background level of reaction, possibly through the sulfur atom in the detergent headgroup with the DTNB. As a final control, we demonstrated that reduction by the aqueous phase-reducing agent DTT resulted in direct conversion of the DTNB, resulting in uniformly high absorbance output (Figure 2F). Representative spectra from several of these samples are shown in Figure 3.

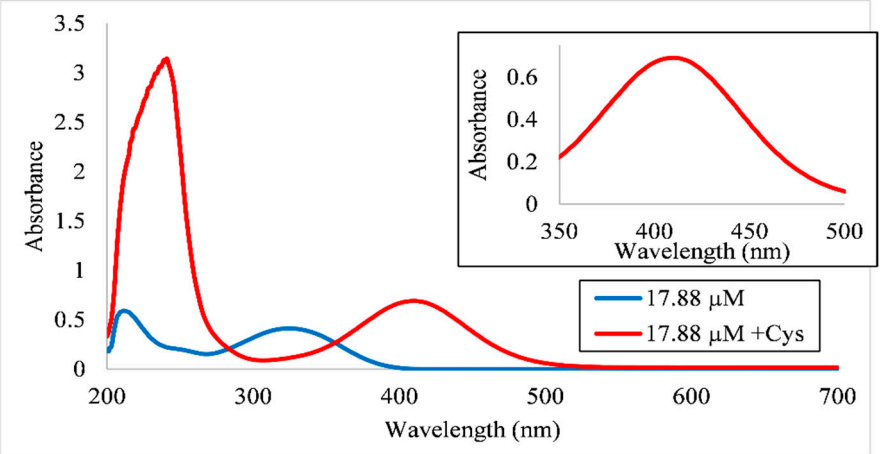


Figure 3. Representative spectra of DTNB in the absence (blue) and presence (red) of free cysteine. The inset shows the zoomed-in region around the peak at 409 nm used in the microplate assays described in Figures 1 and 2.

In addition to the denaturating agents, we also evaluated the impact of added salts on the sample and how this may impact evaluation. The rationale for this is twofold, with the first factor being the acquisition of biological samples, for evaluation in the nanopore-sensing platform will be inherently variable. Specifically, initial experiments on the nanopore platform targeting ovarian cancer biomarkers were evaluated in mock urine samples. In clinical settings, the urine collected from patients will vary in ion levels due to changes in hydration of the patient. The second important role of salts in the sample preparation is regarding the actual nanopore sensor. This platform utilizes a current across an artificial bilayer and utilizes a 3 M KCl solution on either side of the membrane to aid in charge transfer. Thus, we evaluated the ability of the DTNB assay to perform under high salt conditions, as shown in Figure 2E. Again, the assay retained the linear response to free sulfhydryls from Cys, with only a small decrease in sensitivity from 2 M to 3 M added KCl.

3.3. Application to Peptide Model Systems

The utility of the nanopore-sensing assay to detect biomarker peptides relies on the presence of Cys residues in the peptide, but more specifically relies on the presence of Cys residues in the reduced form. The reduced form allows the Cys residue to interact with the gold nanocluster at the center of the sensing mechanism. However, oxidation of Cys residues is a common occurrence, often induced by environmental factors and even by atmospheric oxygen. Thus, the sensitivity of the platform is inherently dependent on the Cys residues being in the appropriate, reduced state before application to the sensor. The reduction of Cys residues by soluble-reducing agents, such as DTT or TCEP, would be incompatible with the sensing platform since removal of those small molecules would be

challenging before application to the sensor. Thus, we sought to evaluate the DTNB assay against a standard peptide in the oxidized form, glutathione, before and after exposure to a reducing gel in which reducing agents are immobilized on the surface of beads. These beads were then physically separated by centrifugation and the glutathione analyzed in the DTNB assay. The assay was performed at pH 8.0 with 1 mM EDTA and 3 M KCl to mimic the conditions used in the sensing platform. The data are shown in Figure 4. The oxidized form of the glutathione (GSSG (ox), red symbols) showed no reactivity with DTNB; however, the oxidized glutathione exposed to the reducing gel (GSSG (ox) + beads, black symbols) demonstrated high reactivity and linear response to the DTNB assay. In order to ensure specificity of the assay, we also evaluated two sulfur-containing amino acids that do not have free thiols. The data for S-methylcysteine (orange) and d-methionine (blue) are also shown in Figure 4.

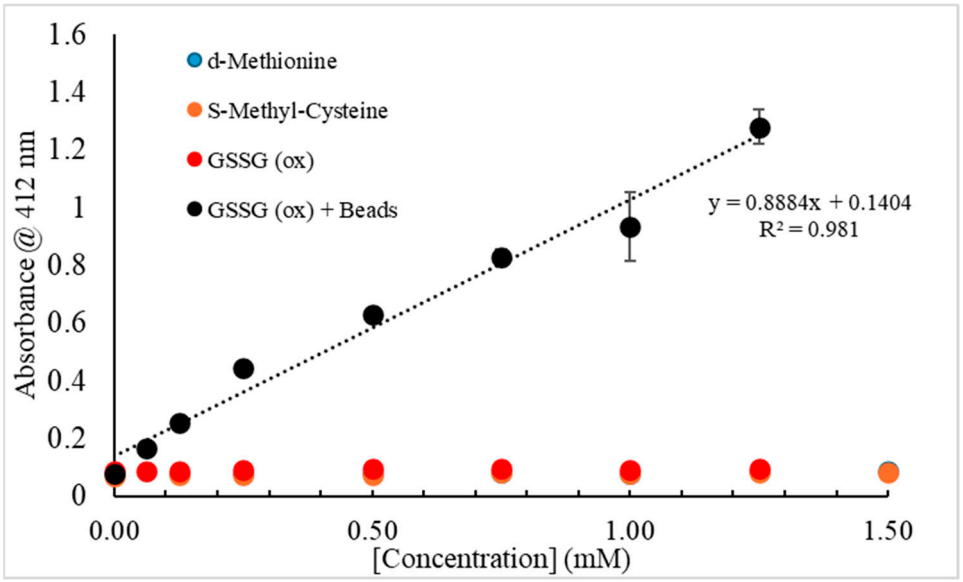


Figure 4. Analysis of GSSG (ox) and non-reactive sulfur-containing amino acids. Glutathione in the oxidized form (GSSG) was analyzed before (red) and after (black) exposure to reducing gel. Non-reactive sulfur-containing amino acids S-methylcysteine (orange) and d-methionine (blue) were analyzed. The data from the three non-reducing samples (blue, red, and orange) overlap on this graph. Data are the average of 3–5 samples, with error bars representing the standard deviation of the samples. In many cases, the error bars are obscured by the symbol size.

Using the conditions described in the earlier assays, we applied them to a series of linear peptide model systems. These peptides represent model sequences and synthetic versions of naturally occurring peptides identified as biomarkers. The peptides were originally analyzed in the nanopore-sensing platform as previously described. The sequences and selected peptide properties are shown in Table 1.

Table 1. Peptide Sequences and Properties.

Name	Amino Acid Sequence	# Amino Acids	Molecular Weight	Net Charge [b]	GRAVY [a]
5C1	CASEW	5	594.64	−1	−0.180
7C1NH$_2$	CLSASEW-NH$_2$	7	793.9	0	0.300
9C5	AESLCASEW	9	995.08	−2	0.044
CP-2	AVYYCQQY	8	1037.15	0	−0.300
IRP2P	RssHCQREEAGGRD*	14	1747.65	1	n/c
Cp20L	WCFGPDGTGPNILTDITKGV	20	2091.37	−1	0.005

[a]: GRand Average of hydropathy, calculated using [32]. [b]: calculated charge at pH 7.0 using (peptidecalculator.net/peptide.aspx). *: s = phosphoserine.

Starting with 1 mg/mL solutions of the peptides, we created a series of peptide test solutions of constant volume to characterize free sulfhydryls under experimental conditions at pH 8 with 1 mM EDTA. Multiple parallel samples were created at several different dilutions based on the original 1 mg/mL stocks of the peptides and subjected to the microplate assay using 3 M KCL in the buffer to mimic the nanopore-sensing assay conditions. The cumulative data are shown in Figure 5. The data shows that the DTNB absorbance is linear for multiple dilutions of the peptides and appears to be linear for all peptides tested. Notably, the concentration ranges tested for these peptides are 10- to 100-fold lower than the conditions noted in the troubleshooting assay development experiments shown above.

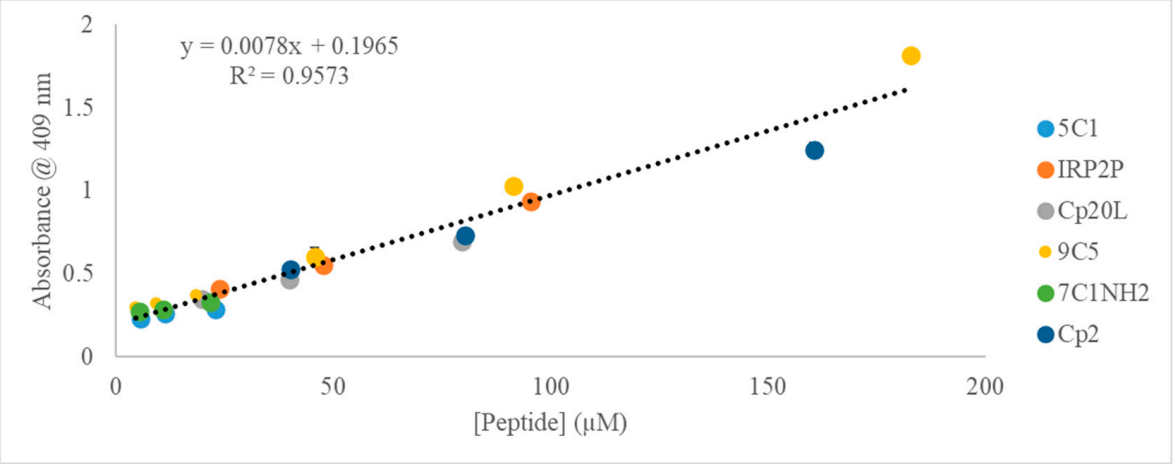


Figure 5. Analysis of multiple peptides by the DTNB microplate assay with 3 M KCl. Peptide stocks were made at 1 mg/mL at pH 8.0 and subsequently diluted to the concentrations shown. The line is a global best fit to all samples and dilutions. Data are the averages of 3–7 independent samples with error bars representing the standard deviation. In most cases, the error bars are obscured by the data markers.

4. Discussion

The DTNB assay for Cys reactivity, commonly referred to as Ellman's assay, is a widely utilized protocol for determining the redox state of sulfhydryl residues in proteins. Since this assay has been well established in the literature for decades, there has been relatively little investigation of the flexibility of the assay or the broad applicability to non-standard reaction conditions. Additionally, Cys reactivity is often directly linked to protein structural changes, which can be assessed via sizing methods, such as SDS-PAGE or mass spectrometry. Together, these factors have left a number of open questions regarding the compatibility of the DTNB assay with additives and non-standard conditions.

The conversion of the traditional DTNB assay protocol to microplate format did not yield any unexpected results. As anticipated, the increase in sample volume in the wells translated to a concomitant increase in absorbance. This can be explained by the increased effective "pathlength" as the volume increases. Using the formula for the volume of a cylinder as our best approximation for pathlength in the wells of the microplate, this translates to a linear increase of 0.26 cm in pathlength per 100 µL additional sample volume. This linear increase is recapitulated in the data in Figure 1B, demonstrating that the volume differences can be directly attributed to effective pathlength.

Importantly, we demonstrate that the DTNB assay is flexible to a variety of sample conditions. The ability of the DTNB assay to retain linear response in the presence of denaturants, such as ethanol, guanidinium HCl, and urea, opens the possibilities to use this method to evaluate protein-folding experiments, specifically targeting the redox state of Cys residues during the denaturation process. This flexibility will also be important when

deploying the nanopore sensor platform to clinical applications, where specific sample preparation conditions may vary based on the biological fluid being tested. Importantly, the concentration of biomarker peptides found in bodily fluids can vary greatly; thus, having robust protocols to ensure these molecules are in the appropriate redox state is critical for optimal sensor output. Since many of the biomarkers in question are found in low nanomolar concentrations in bodily fluids, concentration steps may be necessary in the clinic, and thus, having an assay, which is insensitive to high salt and buffer conditions, is ideal [33–35]. This can add a different dimension to the analysis of protein stability studies, especially in proteins with intrachain disulfide bonds, a common motif in smaller proteins.

5. Conclusions

The data presented demonstrates that the traditional DTNB assay, AKA Ellman's assay, is compatible with a variety of solvent conditions. These solvent conditions allow for flexibility in sample preparation protocols for bioassays that utilize Cys as the diagnostic target of the assay or for protein systems that contain Cys. It also demonstrates the compatibility with solid phase-reducing agents that can ensure appropriate redox state of the peptides for compatibility with the biosensing assay.

Author Contributions: Conceptualization, G.A.C. and J.E.R.; methodology, G.A.C.; investigation, M.L.M., S.R.G., F.G. and M.D.S.; writing—original draft preparation, G.A.C.; writing—review and editing, J.E.R. and M.L.M.; supervision, G.A.C. and J.E.R.; project administration, G.A.C. and J.E.R.; funding acquisition, G.A.C. and J.E.R. All authors have read and agreed to the published version of the manuscript.

Funding: This work was supported by NSF CBET-2011173. F.G. was supported by NIH R25GM119973.

Institutional Review Board Statement: Not applicable.

Informed Consent Statement: Not applicable.

Data Availability Statement: Data is available upon request.

Conflicts of Interest: The authors declare no conflicts of interest.

References

1. Balachandra, S.; Kusin, S.B.; Lee, R.; Blackwell, J.M.; Tiro, J.A.; Cowell, L.G.; Chiang, C.M.; Wu, S.Y.; Varma, S.; Rivera, E.L.; et al. Blood-based biomarkers of human papillomavirus-associated cancers: A systematic review and meta-analysis. *Cancer* **2021**, *127*, 850–864. [CrossRef] [PubMed]
2. Lyman, D.F.; Bell, A.; Black, A.; Dingerdissen, H.; Cauley, E.; Gogate, N.; Liu, D.; Joseph, A.; Kahsay, R.; Crichton, D.J.; et al. Modeling and integration of N-glycan biomarkers in a comprehensive biomarker data model. *Glycobiology* **2022**, *32*, 855–870. [CrossRef] [PubMed]
3. Padilla-Martinez, F.; Wojciechowska, G.; Szczerbinski, L.; Kretowski, A. Circulating Nucleic Acid-Based Biomarkers of Type 2 Diabetes. *Int. J. Mol. Sci.* **2021**, *23*, 295. [CrossRef]
4. Strimbu, K.; Tavel, J.A. What are biomarkers? *Curr. Opin. HIV AIDS* **2010**, *5*, 463–466. [CrossRef]
5. Varesi, A.; Carrara, A.; Pires, V.G.; Floris, V.; Pierella, E.; Savioli, G.; Prasad, S.; Esposito, C.; Ricevuti, G.; Chirumbolo, S.; et al. Blood-Based Biomarkers for Alzheimer's Disease Diagnosis and Progression: An Overview. *Cells* **2022**, *11*, 1367. [CrossRef] [PubMed]
6. Fernandez-Fournier, M.; Lopez-Molina, M.; Torres Iglesias, G.; Botella, L.; Chamorro, B.; Laso-Garcia, F.; Puertas, I.; Tallon Barranco, A.; Otero-Ortega, L.; Frank-Garcia, A.; et al. Antibody Content against Epstein-Barr Virus in Blood Extracellular Vesicles Correlates with Disease Activity and Brain Volume in Patients with Relapsing-Remitting Multiple Sclerosis. *Int. J. Mol. Sci.* **2023**, *24*, 4192. [CrossRef] [PubMed]
7. Dhama, K.; Latheef, S.K.; Dadar, M.; Samad, H.A.; Munjal, A.; Khandia, R.; Karthik, K.; Tiwari, R.; Yatoo, M.I.; Bhatt, P.; et al. Biomarkers in Stress Related Diseases/Disorders: Diagnostic, Prognostic, and Therapeutic Values. *Front. Mol. Biosci.* **2019**, *6*, 91. [CrossRef]
8. Hristova, V.A.; Chan, D.W. Cancer biomarker discovery and translation: Proteomics and beyond. *Expert. Rev. Proteom.* **2019**, *16*, 93–103. [CrossRef]

9. Minutentag, I.W.; Seneda, A.L.; Barros-Filhos, M.C.; de Carvalho, M.; Souza, V.G.P.; Hasimoto, C.N.; Moraes, M.P.T.; Marchi, F.A.; Lam, W.L.; Reis, P.P.; et al. Discovery of Novel miRNAs in Colorectal Cancer: Potential Biological Roles and Clinical Utility. *Non-Coding RNA* **2023**, *9*, 65. [CrossRef]
10. Pessoa, L.S.; Heringer, M.; Ferrer, V.P. ctDNA as a cancer biomarker: A broad overview. *Crit. Rev. Oncol. Hematol.* **2020**, *155*, 103109. [CrossRef]
11. Fritschi, N.; Vaezipour, N.; Buettcher, M.; Portevin, D.; Naranbhai, V.; Ritz, N. Ratios from full blood count as markers for TB diagnosis, treatment, prognosis: A systematic review. *Int. J. Tuberc. Lung Dis.* **2023**, *27*, 822–832. [CrossRef] [PubMed]
12. Kim, M.; Jeong, J.Y.; Seo, A.N. Biomarkers for Predicting Response to Personalized Immunotherapy in Gastric Cancer. *Diagnostics* **2023**, *13*, 2782. [CrossRef]
13. Xie, Q.Y.; Oh, S.; Wong, A.; Yau, C.; Herold, K.C.; Danska, J.S. Immune responses to gut bacteria associated with time to diagnosis and clinical response to T cell-directed therapy for type 1 diabetes prevention. *Sci. Transl. Med.* **2023**, *15*, eadh0353. [CrossRef]
14. Tamborero, D.; Rubio-Perez, C.; Deu-Pons, J.; Schroeder, M.P.; Vivancos, A.; Rovira, A.; Tusquets, I.; Albanell, J.; Rodon, J.; Tabernero, J.; et al. Cancer Genome Interpreter annotates the biological and clinical relevance of tumor alterations. *bioRxiv* **2017**, 140475. [CrossRef] [PubMed]
15. Turewicz, M.; Frericks-Zipper, A.; Stepath, M.; Schork, K.; Ramesh, S.; Marcus, K.; Eisenacher, M. BIONDA: A free database for a fast information on published biomarkers. *Bioinform. Adv.* **2021**, *1*, vbab015. [CrossRef] [PubMed]
16. Wishart, D.S.; Bartok, B.; Oler, E.; Liang, K.Y.H.; Budinski, Z.; Berjanskii, M.; Guo, A.; Cao, X.; Wilson, M. MarkerDB: An online database of molecular biomarkers. *Nucleic Acids Res.* **2021**, *49*, D1259–D1267. [CrossRef]
17. Crosby, D.; Bhatia, S.; Brindle, K.M.; Coussens, L.M.; Dive, C.; Emberton, M.; Esener, S.; Fitzgerald, R.C.; Gambhir, S.S.; Kuhn, P.; et al. Early detection of cancer. *Science* **2022**, *375*, eaay9040. [CrossRef]
18. Hawkes, N. Cancer survival data emphasise importance of early diagnosis. *BMJ* **2019**, *364*, l408. [CrossRef]
19. Howlader, N.; Noone, A.M.; Krapcho, M.; Miller, D.; Brest, A.; Yu, M.; Ruhl, J.; Tatalovich, Z.; Mariotto, A.; Lewis, D.R.; et al. SEER Cancer Statistics Review (CSR) 1975–2018 National Cancer Institute. 2021. Available online: https://seer.cancer.gov/csr/1975_2018/ (accessed on 9 April 2025).
20. Ghimire, M.L.; Cox, B.D.; Winn, C.A.; Rockett, T.W.; Schifano, N.P.; Slagle, H.M.; Gonzalez, F.; Bertino, M.F.; Caputo, G.A.; Reiner, J.E. Selective Detection and Characterization of Small Cysteine-Containing Peptides with Cluster-Modified Nanopore Sensing. *ACS Nano* **2022**, *16*, 17229–17241. [CrossRef]
21. Rockett, T.W.; Almahyawi, M.; Ghimire, M.L.; Jonnalagadda, A.; Tagliaferro, V.; Seashols-Williams, S.J.; Bertino, M.F.; Caputo, G.A.; Reiner, J.E. Cluster-Enhanced Nanopore Sensing of Ovarian Cancer Marker Peptides in Urine. *ACS Sens.* **2024**, *9*, 860–869. [CrossRef]
22. Ellman, G.L. Tissue sulfhydryl groups. *Arch. Biochem. Biophys.* **1959**, *82*, 70–77. [CrossRef]
23. Maeda, H.; Matsuno, H.; Ushida, M.; Katayama, K.; Saeki, K.; Itoh, N. 2,4-Dinitrobenzenesulfonyl fluoresceins as fluorescent alternatives to Ellman's reagent in thiol-quantification enzyme assays. *Angew. Chem. Int. Ed. Engl.* **2005**, *44*, 2922–2925. [CrossRef]
24. Nekrassova, O.; White, P.C.; Threlfell, S.; Hignett, G.; Wain, A.J.; Lawrence, N.S.; Davis, J.; Compton, R.G. An electrochemical adaptation of Ellman's test. *Analyst* **2002**, *127*, 797–802. [CrossRef]
25. Dhawan, S.; Devnani, H.; Babu, J.; Singh, H.; Haider, M.A.; Khan, T.S.; Ingole, P.P.; Haridas, V. Supersensitive Detection of Anions in Pure Organic and Aqueous Media by Amino Acid Conjugated Ellman's Reagent. *ACS Appl. Bio Mater.* **2021**, *4*, 2453–2464. [CrossRef] [PubMed]
26. Guclu, K.; Ozyurek, M.; Gungor, N.; Baki, S.; Apak, R. Selective optical sensing of biothiols with Ellman's reagent: 5,5′-Dithiobis(2-nitrobenzoic acid)-modified gold nanoparticles. *Anal. Chim. Acta* **2013**, *794*, 90–98. [CrossRef] [PubMed]
27. Khan, H.; Khan, K.A.; Khan, M.K.; Ahmad, A.; Niazi, Z.R.; Mangi, A.; Rehman, F.U.; Shah, K.U.; Gul, R.; Jan, S.U. Thiol-disulfide exchange reactions occurring at modified bovine serum albumin detected using ellman's reagent (5, 5′-dithiobis (2-itrobenzoic acid). *Pak. J. Pharm. Sci.* **2020**, *33*, 2767–2772. [PubMed]
28. Sinko, G.; Calic, M.; Bosak, A.; Kovarik, Z. Limitation of the Ellman method: Cholinesterase activity measurement in the presence of oximes. *Anal. Biochem.* **2007**, *370*, 223–227. [CrossRef]
29. Zhu, J.; Dhimitruka, I.; Pei, D. 5-(2-Aminoethyl)dithio-2-nitrobenzoate as a more base-stable alternative to Ellman's reagent. *Org. Lett.* **2004**, *6*, 3809–3812. [CrossRef]
30. Riddles, P.W.; Blakeley, R.L.; Zerner, B. Reassessment of Ellman's reagent. *Methods Enzymol.* **1983**, *91*, 49–60. [CrossRef]
31. Kraus, D. Consolidated data analysis and presentation using an open-source add-in for the Microsoft Excel® spreadsheet software. *Med. Writ.* **2014**, *23*, 25–28. [CrossRef]
32. Kyte, J.; Doolittle, R.F. A simple method for displaying the hydropathic character of a protein. *J. Mol. Biol.* **1982**, *157*, 105–132. [CrossRef] [PubMed]
33. Bhensdadia, N.M.; Hunt, K.J.; Lopes-Virella, M.F.; Michael Tucker, J.; Mataria, M.R.; Alge, J.L.; Neely, B.A.; Janech, M.G.; Arthur, J.M. Urine haptoglobin levels predict early renal functional decline in patients with type 2 diabetes. *Kidney Int.* **2013**, *83*, 1136–1143. [CrossRef] [PubMed]

34. El Atab, O.; Gupta, B.; Han, Z.; Stribny, J.; Asojo, O.A.; Schneiter, R. Alpha-1-B glycoprotein (A1BG) inhibits sterol-binding and export by CRISP2. *J. Biol. Chem.* **2024**, *300*, 107910. [CrossRef] [PubMed]
35. Kentsis, A.; Ahmed, S.; Kurek, K.; Brennan, E.; Bradwin, G.; Steen, H.; Bachur, R. Detection and diagnostic value of urine leucine-rich alpha-2-glycoprotein in children with suspected acute appendicitis. *Ann. Emerg. Med.* **2012**, *60*, 78–83.e1. [CrossRef]

Disclaimer/Publisher's Note: The statements, opinions and data contained in all publications are solely those of the individual author(s) and contributor(s) and not of MDPI and/or the editor(s). MDPI and/or the editor(s) disclaim responsibility for any injury to people or property resulting from any ideas, methods, instructions or products referred to in the content.